Transmission through subwavelength slit structures with a double period: a simple model for the prediction of resonances

2009 J. Opt. A: Pure Appl. Opt. 11 105102

(http://iopscience.iop.org/1464-4258/11/10/105102)

J. Opt. A: Pure Appl. Opt. **11** (2009) 105102 (8pp) doi:10.1088/1464-4258/11/10/105102

Transmission through subwavelength slit structures with a double period: a simple model for the prediction of resonances

Diana C Skigin

Grupo de Electromagnetismo Aplicado, Departamento de Física, Facultad de Ciencias Exactas y Naturales, Universidad de Buenos Aires, Ciudad Universitaria, Pabellón I, C1428EHA Buenos Aires, Argentina
and
Consejo Nacional de Investigaciones Científicas y Técnicas (CONICET), Avenida Rivadavia 1917, C1033AAJ Buenos Aires, Argentina

E-mail: dcs@df.uba.ar

Received 4 March 2009, accepted for publication 26 June 2009
Published 10 August 2009
Online at stacks.iop.org/JOptA/11/105102

Abstract
Transmission wire gratings comprising several subwavelength slits within each period (compound gratings) have been shown to exhibit abrupt dips in the transmission response. These minima correspond to phase resonances, that are excited in the structure when a particular distribution of the magnetic field phases inside the slits is generated. By using an approximate model based on the modal method, we can easily obtain the resonant frequencies which correspond to transmittance maxima (Fabry–Perot resonances) and minima (phase resonances). This simplified model constitutes a practical tool to accurately predict the relevant characteristics of the transmitted response of compound structures for normal and oblique incidence, without a full solution of the scattering problem.

Keywords: enhanced transmission, nanogratings, resonances, photonic crystals

1. Introduction

The transmitted response of a periodic array of rectangular slits presents a series of Fabry–Perot (FP) resonances, which manifest themselves as transmittance maxima for certain wavelengths. The origin of these resonances lies in the excitation of waveguide modes within each individual slit, and their location is related to the thickness of the structure. This problem has been studied by Porto *et al* [1], where the authors also analyze the physical origin of such transmission resonances as a function of the thickness of the structure and of the slit width by using a simplified model.

One-dimensional metallic structures have been widely investigated in the last decade in connection with the enhanced transmission phenomenon first reported in a metallic plate with holes [2]. Theoretical [1, 3–11] as well as experimental [12–16] research has been carried out in connection with slit structures and their capability of producing enhanced transmission.

Dual-period structures formed by slit arrays have only attracted the attention of a few authors since very recently, although they provide more degrees of freedom than regular gratings for the design of the transmitted response. Examples of their potential are the possibility of intensification and/or cancelation of a given diffraction order [17–19] and the excitation of phase resonances [20]. It has been shown that transmission metallic gratings comprising several subwavelength slits within each unit cell exhibit phase resonances, i.e., resonances that are characterized by a phase reversal of the magnetic field in adjacent slits within each period [20–23]. Such resonances only take place under p-polarized incidence (electric field in the plane of incidence), and are only permitted when there is more than one slit or cavity within each period. In the regular grating case, the pseudoperiodicity condition of the fields imposes that all periods of the grating are equivalent, thus forbidding different field phases in adjacent slits, which is the basic requirement for a phase resonance.

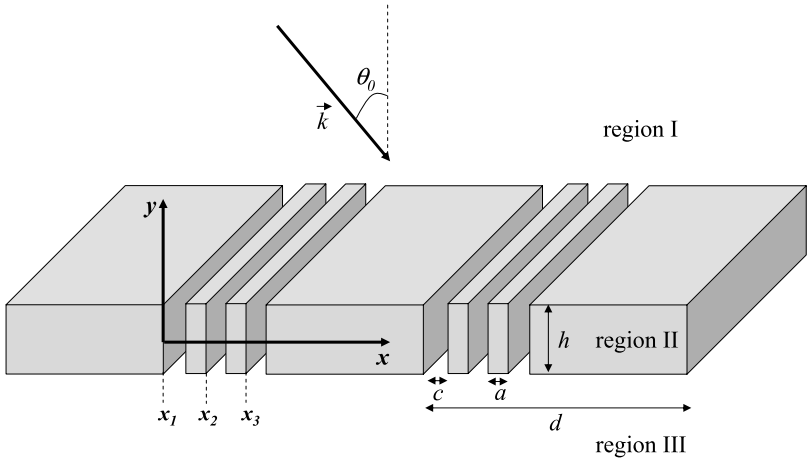

Figure 1. Scheme of the compound structure with subwavelength slits.

Only a few recent works reported experimental demonstrations of phase resonances in slit structures. Hibbins *et al* measured the transmissivity of an air-filled compound grating comprised of two narrow slits flanking a wider central slit under microwave radiation [24] and confirmed the existence of a dip within a FP peak, which is characteristic of phase resonances. Ma *et al* also reported measurements for periodic structures with unit cells consisting of two or three slits of different widths, and found clear evidence of phase resonances in the microwave regime [25]. Recently, Navarro-Cía *et al* reported the measurement of the transmittance for structures with one, two and three slits per period in an aluminum plate, and have demonstrated the existence of phase resonances in the millimeter wave regime [26].

In this work an approximate model—based on the classical modal method [27] extended to deal with dual-period metallic structures with subwavelength slits [20]—is developed, which predicts the wavelengths at which a transmittance minimum is found, i.e., the spectral location of phase resonances. This model also allows the determination of the frequencies at which the maxima connected with the FP resonances of each single slit are found. Thus, the relevant information regarding the response of double-period subwavelength slit structures is obtained via a very simple approach and then the computation time required for the overall calculation decreases considerably. Very recently, another model for the prediction of enhanced transmission and phase resonances in compound structures has been presented [28, 29], where the authors show that simple reasoning starting from standard transmission line and waveguide theory provides a useful tool to qualitatively and quantitatively predict the behavior of slits systems, and also accounts for all of the reported phenomena. The basic idea of this model is to reduce the real problem to the evaluation of the scattering of a TEM wave supported by a parallel plate transmission line when a finite length section of another parallel plate transmission line having much higher characteristic admittance is inserted, and the influence of below cutoff modes is accounted for by an equivalent capacitance. This approach is completely different from that presented here, in which the rigorous modal method with the single mode approximation is applied to solve the scattering problem.

In section 2 a p-polarized plane wave impinging on a double-period slit structure is considered, and the modal approach developed to predict the resonances is outlined. The results obtained with this method are given in section 3, where the transmitted intensity and the modal amplitudes within the slits are shown as a function of the incident wavelength. Dispersion diagrams for the double-period slit structure obtained by the simple model proposed are also shown. The conclusions of the work are summarized in section 4.

2. Approximate modal method

Consider the double-period structure of figure 1 comprising perfectly conducting wires of rectangular cross section and subwavelength slits of width c and depth h. Each period d comprises several wires and J slits, forming a subgrating. For in-plane incidence, the basic polarization modes are uncoupled, and then the complete vectorial diffraction problem can be separated into two scalar problems for E_z (s polarization) and H_z (p polarization), from which the other components of the electromagnetic field can be obtained.

Consider a p-polarized plane wave (magnetic field along the wires) of wavelength λ impinging on the wire array, which is immersed in vacuum. The problem is divided into three regions, and the modal approach consists of expanding the fields in each region in their own eigenfunctions, which satisfy the boundary conditions. In regions I ($y \geqslant h/2$) and III ($y \leqslant -h/2$) the tangential magnetic field is expressed as:

$$H_z^{\mathrm{I}}(x, y) = \exp\left[\mathrm{i}(\alpha_0 x - \beta_0(y - h/2))\right] + \sum_n R_n \exp\left[\mathrm{i}(\alpha_n x + \beta_n(y - h/2))\right], \quad (1)$$

$$H_z^{\mathrm{III}}(x, y) = \sum_n T_n \exp\left[\mathrm{i}(\alpha_n x - \beta_n(y + h/2))\right], \quad (2)$$

where

$$\alpha_n = \frac{2\pi}{\lambda}\sin\theta_0 + n\frac{2\pi}{d}, \quad (3)$$

$$\beta_n^2 = \left(\frac{2\pi}{\lambda}\right)^2 - \alpha_n^2, \tag{4}$$

θ_0 is the angle of incidence, i is the imaginary unit, and R_n and T_n are the unknown reflected and transmitted Rayleigh amplitudes, respectively.

In region II ($|y| \leqslant h/2$), there are two zones: the perfect conductor and the slits. Since we are considering slits whose width is much smaller than the incident wavelength, the field within each slit can be approximated by the fundamental mode only, which for p polarization corresponds to a constant field in the x direction:

$$H_{zj}^{\mathrm{II}}(x, y) = a_j \cos[ky] + b_j \sin[ky], \tag{5}$$

where $k = \omega/c$ is the propagation constant in vacuum, ω is the incident frequency and c is the speed of light in vacuum. The subscript j denotes the slit within each period, and a_j and b_j are the unknown modal amplitudes.

By applying the boundary conditions at the interfaces between regions, i.e., the continuity of the tangential electric and magnetic fields in the vacuum–vacuum interfaces and the requirement of null tangential electric field on the perfectly conducting surface of the wires, four x-dependent equations are obtained. These equations are projected on convenient bases to remove the spatial dependence, and this leads to the following equations for the unknown reflected, transmitted and modal amplitudes:

$$\sum_n T_n \mathrm{e}^{\mathrm{i}\alpha_n x_j} F_n^+ = c[\tilde{a}_j - \tilde{b}_j], \tag{6}$$

$$\sum_n (\delta_{n0} + R_n)\mathrm{e}^{\mathrm{i}\alpha_n x_j} F_n^+ = c[\tilde{a}_j + \tilde{b}_j], \tag{7}$$

$$\sum_j k\mathrm{e}^{-\mathrm{i}\alpha_n x_j}[\tilde{a}_j D_2 + \tilde{b}_j D_1]F_n^- = -\mathrm{i}dT_n\beta_n, \tag{8}$$

$$\sum_j k\mathrm{e}^{-\mathrm{i}\alpha_n x_j}[-\tilde{a}_j D_2 + \tilde{b}_j D_1]F_n^- = \mathrm{i}d(-\delta_{n0} + R_n)\beta_n, \tag{9}$$

where

$$\tilde{a}_j = a_j \cos(kh/2), \tag{10}$$

$$\tilde{b}_j = b_j \sin(kh/2), \tag{11}$$

$$F_n^{\pm} = \int_0^c \mathrm{e}^{\pm\mathrm{i}\alpha_n x}\,\mathrm{d}x, \tag{12}$$

$$D_1 = \operatorname{cotan}(kh/2), \tag{13}$$

$$D_2 = \tan(kh/2). \tag{14}$$

The reflected and transmitted amplitudes are eliminated from the system formed by equations (6)–(9), and two matrix equations are obtained, whose solutions are the modal amplitudes:

$$\tilde{a}_j = \sum_{j'} -(A^{-1})_{jj'} I_{j'} \tag{15}$$

$$\tilde{b}_j = \sum_{j'} (B^{-1})_{jj'} I_{j'}, \tag{16}$$

where

$$A_{jj'} = \mathrm{i}\frac{k}{d} D_2 \phi_{jj'} - c\delta_{jj'}, \tag{17}$$

$$B_{jj'} = \mathrm{i}\frac{k}{d} D_1 \phi_{jj'} + c\delta_{jj'}, \tag{18}$$

$$I_{j'} = F_0^+ \mathrm{e}^{\mathrm{i}\alpha_0 x_{j'}}, \tag{19}$$

$$\phi_{jj'} = \sum_n \mathrm{e}^{\mathrm{i}\alpha_n (x_j - x_{j'})} \frac{F_n^+ F_n^-}{\beta_n}, \tag{20}$$

and x_j denotes the position of the left wall of the jth slit.

Once the modal amplitudes are found using equations (15) and (16), the reflected and transmitted amplitudes can also be computed to get the electromagnetic field everywhere. Instead of solving the above equations, in what follows we focus on the matrices A and B—whose elements are $A_{jj'}$ and $B_{jj'}$, respectively—obtained by the approximate model, and analyze them to extract information about the resonances of the compound slit system without a previous solution of the diffraction problem.

3. Results

In this section we analyze slit structures with one, two, three and five slits per period. In all cases, the results have been obtained by the approximate model outlined in section 2 for incident p polarization. The zero-order transmittance curves have been compared with those obtained by the modal method without the assumption of a single mode expansion within the slits [23], and an excellent agreement was found, which confirms the validity of the simple model.

The results shown in figure 2 correspond to a simple grating, i.e., a periodic array with a single slit in each period. The parameters of the structure are: $c/d = 0.08$, $h/d = 1.14$, $\theta_0 = 0°$. As expected for regular slit gratings, FP resonances appear as peaks in the zero-order transmitted response (figure 2(a)) [1]. In the wavelength range considered, these resonances are found approximately at $\lambda/d = 1.279$ and 2.512. Taking into account that the waveguide resonances for an infinitely narrow slit are given by $\lambda_m/d = (2h/d)/m$ (with m being a positive integer), for the thickness considered in this example those values are $\lambda_1/d = 2.28$ and $\lambda_2/d = 1.14$. Then, the peak at $\lambda/d = 2.512$ can be associated with the first mode ($m = 1$) and that at $\lambda/d = 1.279$ to the second mode ($m = 2$). As already observed in previous works [3, 4, 30], the spectral positions of FP resonances are affected by the finite width of the slits among other parameters, and then there is a shift between the predicted and the calculated values. The $m = 1$ peak corresponds to half a wavelength fitting in the depth of the slit ($h = \lambda/2$). In a simplified approach, the magnetic field within each slit at resonance can be regarded as a stationary wave with nodes at the $y = \pm h/2$ interfaces. Then, the magnetic field has an even distribution along y for the $m = 1$ mode, and according to equation (5) this suggests that the modal amplitude a_1 and the matrix A are the relevant quantities in this case. On the other hand, for the $m = 2$ resonance the magnetic field has an odd distribution along the coordinate y, and then it is expected that the amplitude b_1 and the matrix B govern the behavior in this case. These characteristics can be observed in figure 2(b): the absolute value of the amplitude $\tilde{a}_1$ has a peak at the $m = 1$ resonance

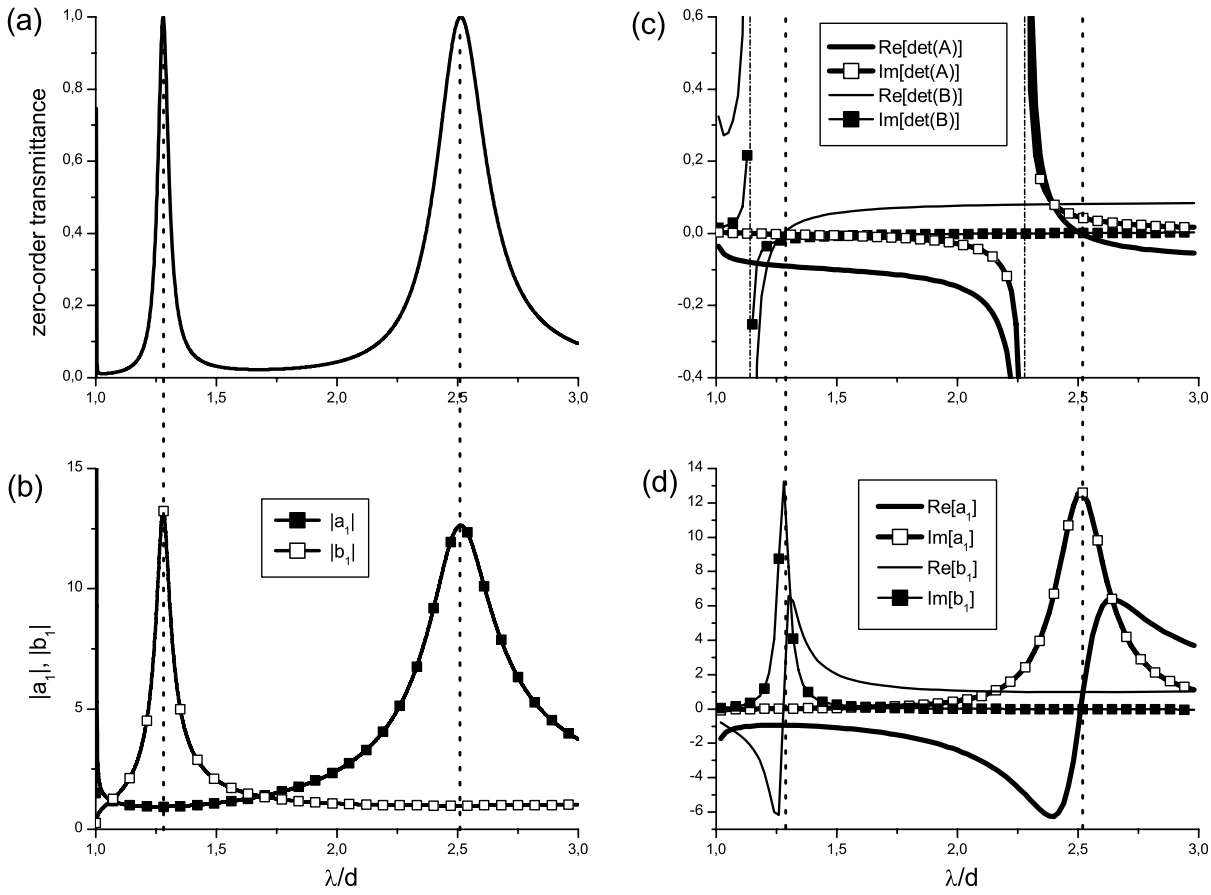

Figure 2. Simple structure with a single slit of width $c/d = 0.08$ and depth $h/d = 1.14$ within each period under normal incidence. (a) Zero-order transmittance as a function of the wavelength-to-period ratio λ/d; (b) absolute value of the modal amplitudes; (c) real and imaginary parts of the determinant of matrices A and B; (d) real and imaginary parts of the modal amplitudes a_1 and b_1.

($\lambda/d = 2.512$), whereas $|\tilde{b}_1|$ has a peak at the $m = 2$ resonance ($\lambda/d = 1.279$).

According to equations (17) and (18), in the simple grating case, A and B are 1×1 matrices ($j = j' = 1$) and then $A = \det(A) = A_{11}$ and $B = \det(B) = B_{11}$. From equations (15) and (16) and using (17)–(20) we get the following expressions for the modal amplitudes under normal incidence:

$$\tilde{a}_1 = -\frac{c}{A_{11}}, \tag{21}$$

$$\tilde{b}_1 = \frac{c}{B_{11}}. \tag{22}$$

Since FP resonances are associated with an intensification of the field inside the slits, the resonant wavelengths are those that minimize the absolute value of the denominator in (21) and (22). Under normal incidence, approximate analytical expressions for B_{11} and A_{11} can be derived. In what follows we focus on the analysis of the $m = 2$ resonance, i.e., on matrix B and modal amplitudes $\tilde{b}_j$ (the procedure for the $m = 1$ resonance is completely analogous).

To obtain the expression for B_{11} only the first three terms in the sums over n in equations (1) and (2) have been retained, which correspond to the 0 and ± 1 reflected and transmitted orders:

$$B_{11} = \frac{2}{\sqrt{\lambda^2 - d^2}} \operatorname{cotan}(kh/2) \left| \frac{e^{i2\pi c/d} - 1}{i2\pi/d} \right|^2 + c + i\frac{c^2}{d} \operatorname{cotan}(kh/2). \tag{23}$$

It is clear from this expression that the real and imaginary parts of B_{11} have asymptotes at $kh/2 = q\pi$, (q integer), which in the wavelength range considered in figure 2 corresponds to $\lambda/d = h/d = 1.14$—similarly, A_{11} has asymptotes at $kh/2 = (2q + 1)\pi$, i.e., at $\lambda/d = 2h/d = 2.28$ within the interval under consideration. In figure 2(c), the real and imaginary parts of the determinants of A and B are plotted as a function of λ/d, and the asymptotes are marked by dash–dotted lines. As expected, no resonances are found at these wavelengths. On the other hand, it can be noticed that the minimum of the absolute value of the determinant is found when its real part vanishes: $\mathrm{Re}[\det(A)] = 0$ at the $m = 1$ resonance and $\mathrm{Re}[\det(B)] = 0$ at the $m = 2$ resonance ($\mathrm{Re}[\cdot]$ denotes real part). This seems to be a characteristic of the dependence of the resulting equations on the wavelength for slits systems. This kind of behavior has already been reported by other authors for simple gratings [1, 31], and they found that there is a close correspondence between the transmittance maxima and the spectral positions of the zeros of the real

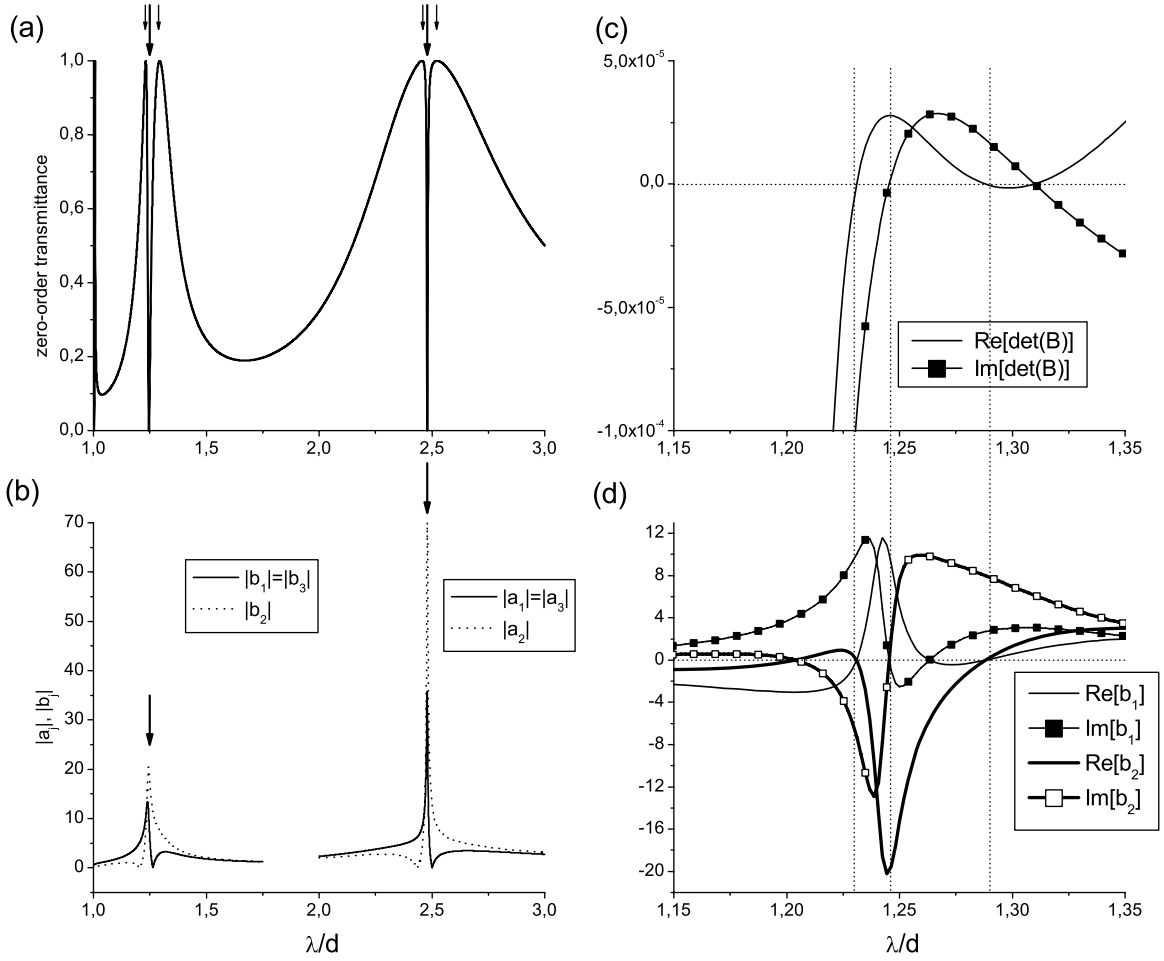

Figure 3. Compound structure with three slits of $c/d = a/d = 0.08$ and $h/d = 1.14$ within each period under normal incidence. (a) Zero-order transmittance as a function of the wavelength-to-period ratio λ/d; (b) absolute value of the modal amplitudes; (c) real and imaginary parts of the determinant of matrix B; (d) real and imaginary parts of the modal amplitudes b_1 and b_2.

or the imaginary part of a certain function. In particular, Quémerais *et al* [31] found that waveguide resonances occur at the minima of a certain denominator, and that those values are approximately reached when its real part vanishes, the width of the resonance being proportional to its imaginary part.

It is interesting to notice in figure 2(d) that at the resonant wavelengths, at which the absolute values of a_1 and b_1 have peaks, the imaginary parts of the modal amplitudes are maximized and, at the same time, their real parts vanish: $\mathrm{Re}[\tilde{b}_1] = 0$ at the $m = 2$ resonance (thin solid line) and $\mathrm{Re}[\tilde{a}_1] = 0$ at the $m = 1$ resonance (thick solid line). From equation (22) $B_{11}\tilde{b}_1 = c$. Taking into account that $c \in \Re$, if $\mathrm{Re}[B_{11}] = 0$ then $\mathrm{Re}[\tilde{b}_1] = 0$, as observed in figure 2(d). Physically, the fact that at resonance $\tilde{b}_1 \in \Im$ implies that the field within the slits is in phase with the incident wave. For any other wavelength $\tilde{b}_1$ is complex with nonzero real and imaginary parts, and there is a phase shift between the incident wave and the slit field.

In figure 3 we show results for a compound structure with three slits per period, as schematized in figure 1. The width of the slits is $c/d = 0.08$, the separation between adjacent slits is $a/d = 0.08$ and their depth is $h/d = 1.14$. As already reported in earlier works [20, 22, 23, 26], the zero-order transmittance exhibits sharp dips within each FP resonance peak (see figure 3(a)). The physical origin of these dips can be explained in terms of phase resonances, which are generated by a particular arrangement of the magnetic field phases within the slits [20, 32–34]. If the grating comprises several slits in the period (compound grating), the distribution of field phases in the slits can have different configurations, not allowed in simple gratings due to the pseudoperiodic property. In the three-slits case and under normal illumination, the only phase configuration allowed (other than having equal phases in all the slits) is the one known as the π-mode [32]; this resonance is characterized by a phase reversal between the central and the external slits, and it is also called the $(+-+)$ mode.

In figure 3(a), it is shown that these dips are found at $\lambda/d = 1.2458$ and at $\lambda/d = 2.4792$, i.e., within the FP resonant peaks. As observed in figure 3(b), the modal amplitudes in the three slits are maximized in the vicinity of the resonances. In particular, $\tilde{a}_j$ have a prominent role near the $m = 1$ resonance, and $\tilde{b}_j$ at the $m = 2$ resonance—the bold arrows in figures 3(a) and (b) mark the spectral positions of the dips and the thin short ones denote the maxima positions. As expected due to the symmetry imposed by the normal incidence, the amplitudes at both external slits are equal.

Table 1. Spectral positions λ/d of transmission maxima, transmission minima, and zeros of the real and imaginary parts of the determinant of matrices A and B for one to three slits per period structures with the same parameters as figures 2 and 3.

	Transmittance maxima	Transmittance minima	α_{rA} = Zeros of Re[det(A)]	α_{iA} = Zeros of Im[det(A)]	α_{rB} = Zeros of Re[det(B)]	α_{iB} = Zeros of Im[det(B)]
1 slit	1.279	—	2.51	1.14	1.28	2.28
	2.512					
2 slits	1.294	—	2.502	1.14	1.264	1.264
	2.52		2.522	2.502	1.294	2.28
3 slits	1.232	*1.24588*	2.454	1.14	1.232	*1.246*
	1.293	*2.4792*	2.516	*2.48*	1.29	1.31
	2.455		2.568	2.568	1.31	2.28
	2.522					

Approximate expressions for the modal amplitudes can be obtained by retaining only the terms with $n = 0$ and ± 1 in the series of transmitted and reflected fields. However, it is important to remark that if all of the evanescent waves are neglected, i.e., only the propagating specular and forward orders are considered in the calculation, the transmitted response does not reproduce the dips but only the peaks, which moreover, appear significantly shifted with respect to their actual spectral position. This suggests that the generation of phase resonances is intimately connected with the existence of evanescent waves along the structure.

In figure 3(c), we plot the real and imaginary parts of the determinant of matrix B in the wavelength range $1.15 \leqslant \lambda/d \leqslant 1.35$, i.e., in the vicinity of the $m = 2$ FP resonance, and in figure 3(d) the real and imaginary parts of the modal amplitudes $\tilde{b}_j$ in the three slits are shown in the same interval. The vertical dotted lines denote the relevant spectral positions: those at $\lambda/d = 1.232$ and 1.293 mark the transmission maxima, and that at $\lambda/d = 1.246$ marks the transmission dip. It can be observed that for the resonant wavelengths that give transmission peaks, the real part of the determinant of matrix B vanishes at those wavelengths. This means that the rule found for the location of FP resonances in simple structures can also be applied to compound structures. At the same time, the real parts of the modal amplitudes $\tilde{b}_j$ of all of the three slits vanish, producing purely imaginary modal amplitudes, as occurs for a structure with a single slit per period. Conversely, at the phase resonance which gives the transmittance dip, the imaginary part of the determinant of matrix B is null and the imaginary parts of the modal amplitudes $\tilde{b}_j$ also vanish. Then, at the phase resonance the $\tilde{b}_j$ are purely real and $\tilde{b}_1 = \tilde{b}_3$ has the opposite sign to $\tilde{b}_2$, meaning that the fields in adjacent slits are phase reversed. The same behavior is found for the determinant of matrix A and the modal amplitudes $\tilde{a}_j$ near the $m = 1$ resonance (not shown). This constitutes one of the main results of the present work.

In table 1 we list the spectral positions of the transmitted maxima and minima, and the zeros of the real and imaginary parts of the determinant of matrices A and B for structures with one, two and three slits per period with the same geometrical parameters considered in figures 2 and 3 under normal incidence. We denote these zeros by α_{sF}, where s = r, i denotes real and imaginary part, respectively, and $F = A$ or B denotes the matrix. It is evident that there is a close correspondence between them: the transmittance maxima are correlated with the zeros of the real part of the determinants (α_{rA} and α_{rB}) in the one-, two-, and three-slit systems, whereas the transmission dips—only present in the three-slits case under normal incidence—are related to the zeros of the imaginary part of the determinants. As expected, the features in the vicinity of the $m = 1$ resonance are related to matrix A whereas those close to the $m = 2$ resonance are related to matrix B. Notice that in table 1 there are other zeros that cannot be associated neither with maxima nor with minima in the transmittance response, whose values are: $\lambda/d = 1.14$ and 2.28 (for the system with a single slit per period), $\lambda/d = 1.14$, 1.264, 2.28, 2.502 for the system with two slits per period, and $\lambda/d = 1.14$, 1.31, 2.28, 2.568 for the three-slits case. As discussed above in connection with the single-slit system, det(A) and det(B) have asymptotes at certain wavelengths at which Im[det(B)] and Im[det(A)] have zeros, mainly governed by the cotan($kh/2$) and tan($kh/2$) functions that appear in the explicit expressions of det(B) and det(A), respectively. In table 1 the zeros at $\lambda/d = 1.14$ and 2.28 are of this type. This kind of zero is also found as the number of slits is increased, and additionally, for structures with more than one slit per period, there are certain wavelengths at which the real and imaginary parts of the determinants vanish simultaneously, i.e., that are zeros of the absolute value of the determinant, which in this example are found at $\lambda/d = 1.264$, 1.31, 2.502 and 2.568. These asymptotes and zeros are a consequence of the single mode approximation used in the present work. They do not represent a singular behavior of the structure at those wavelengths, but a limitation of the approach, which permits us to uncouple the equations for the modal amplitudes, but, at the same time, introduces non-physical singularities. Therefore, they should not be taken into account for the detection of resonances of the system. According to our results for normal incidence, the transmittance maxima appear at α_{rA} and at α_{rB} and the transmittance minima at α_{iA} and at α_{iB} provided these values do not correspond either to asymptotes or to zeros of the absolute value of the determinant of any of the matrices A or B.

The zeros of the real and imaginary parts of the determinants could then be used to predict the spectral positions of the FP resonances as well as of the phase resonances in double-period slit structures, without having to solve the complete scattering problem, which implies matrix inversions and consequently, more computation time. To further investigate the validity of this result for non-normal

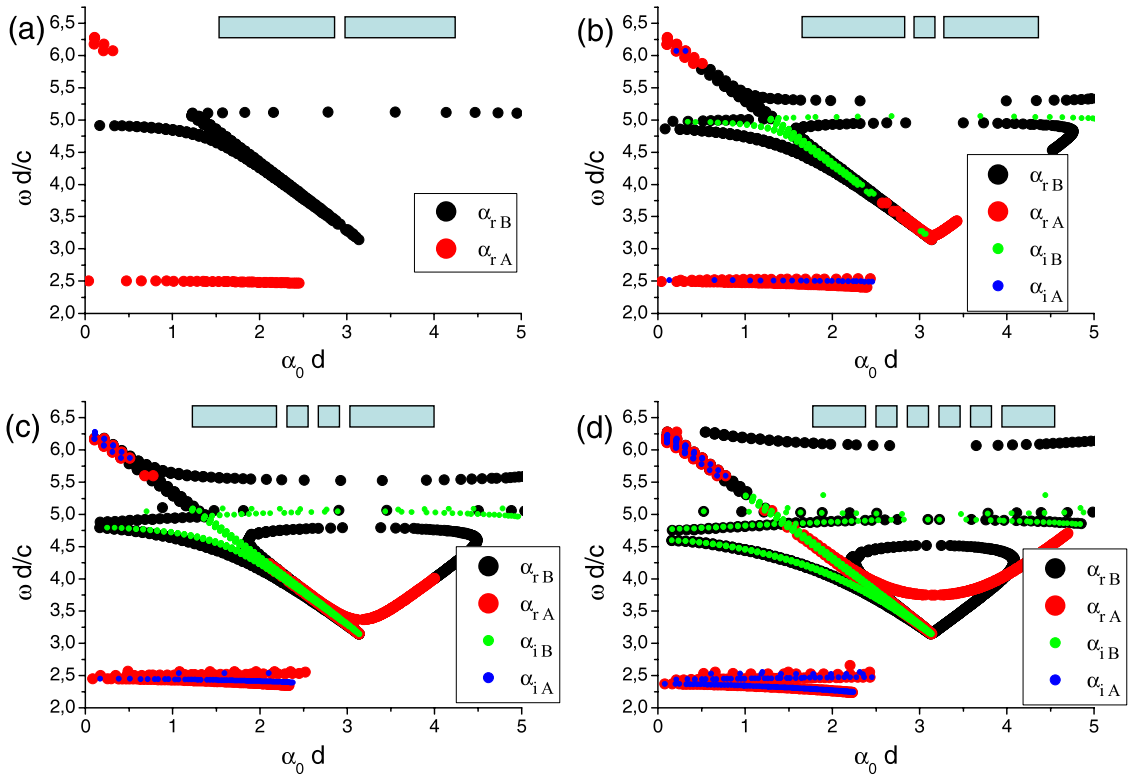

Figure 4. Zeros of the real and imaginary parts of the determinant of matrices A and B as a function of the x-component of the incident wavevector $\alpha_0\ d$ and of the normalized frequency, for structures with different numbers of slits in the period, as schematized in the insets of each panel. (a) $J = 1$; (b) $J = 2$; (c) $J = 3$; (d) $J = 5$.

(This figure is in colour only in the electronic version)

incidence, we show in figure 4 the zeros of the real and imaginary parts of the determinant of matrices A and B as a function of the x-component of the incident wavevector $\alpha_0 d$ and of the normalized frequency, for structures with one, two, three and five slits per period, with the same parameters considered in the previous figures (the zeros of the absolute values of the determinants and those coincident with asymptotes have been omitted for the sake of clarity). These four figures are to be compared with figure 4 of [22], where the transmitted intensity is plotted as a function of the same two variables, and for the same structures. In that figure, the white zones represent maximum transmittance and the black ones represent transmittance minima. Then, it is expected for the positions of the zeros of the real part of the matrix determinants, which are associated with the transmittance maxima, to be coincident with the white zones in figure 4 of [22]. On the other hand, the positions of the zeros of the imaginary part of the matrix determinants, which are associated with the transmittance dips, are expected to agree with the black zones in figure 4 of [22].

In figure 4(a) only the zeros of the real parts are plotted (α_{rA}, red circles and α_{rB}, black circles), since no transmittance dips are present in the case of a single slit per period. From comparison with figure 4(a) of [22] it can be observed that these zeros describe the permitted bands, which correspond to the transmittance maxima positions and are associated with the waveguide resonances. As already observed in regular slits systems [1], this kind of resonance is weakly dependent on the incidence angle θ_0, and therefore they appear as flat bands. In this case, the permitted bands cut the frequency axis at $\omega d/c \approx 2.5$ and 5, which correspond to the peaks at $\lambda/d \approx 2.5$ and 1.25 observed in figure 2(a) for normal incidence. It is important to remark that this plot represents the behavior of the structure under oblique incidence, and that even for this general case the values of α_{rA} and α_{rB} predict very accurately the maxima positions. Besides, this plot provides us with additional information concerning the resonances: the red circles are connected with an even resonant mode since the matrix A, whose determinant is responsible for the zeros α_{rA}, is associated with the $\cos(ky)$ dependence of the magnetic field (see equations (5) and (15)). On the other hand, the black circles, which are associated with matrix B, represent an odd dependence of the form $\sin(ky)$, according to equations (5) and (16).

Figure 4(b) corresponds to a compound structure with two slits in each period. As reported in previous works [22, 26], the transmittance response for normal incidence is similar to that of a one-slit system, whereas a dip is found within each FP peak when the illumination is no longer normal. These dips are represented by the blue and green circles in figure 4(b), which correspond to α_{iA} and α_{iB}, respectively. These zeros describe a narrow forbidden band, which coincides with the dark narrow band observed within each bright region in figure 4(b) of [22]. No zeros (blue or green circles) were found on the ordinates axis (for $\alpha_0 d = 0$), which means that

these minima in the transmission response are forbidden for normal incidence. Besides, our simple model also provides information about which modal amplitude resonates at each frequency. Consistently with the results of figure 4(a) for a simple grating, α_{rA} (red circles) and α_{rB} (black circles) give the positions of the transmittance maxima.

As the number of slits per period increases, the transmitted response becomes more complex, with more dips and peaks. In this case, a transmission minimum appears within each maximum even for normal incidence. For the off-normal situation, one more dip is found within each transmission peak, which can be identified as a narrow dark band within the bright zone in figure 4(c) of [22]. In figure 4(c) of the present work, the calculated zeros α_{sF} for a structure with three slits per period are shown, and it can be observed that the characteristics already observed in the transmitted response (figure 4(c) of [22]) are also evidenced. The minima, represented by the zeros α_{iA} and α_{iB} (blue and green circles), describe very accurately the spectral positions of the dips. Also, the new forbidden bands that appear for non-normal incidence can also be identified as new lines of blue and green circles in the present results. Finally, for five slits per period, more forbidden bands are found in the transmittance response, and this behavior is also observed in the spectral positions of the zeros in this case (figure 4(d)).

4. Conclusions

A simple model for the treatment of the diffraction problem from a double-period slits structure has been developed, which predicts the spectral positions of the transmittance maxima, governed by FP resonances within the slits, and of the transmittance minima, corresponding to the excitation of phase resonances. The approximate model incorporates two assumptions to the exact classical modal method: first, the metal is considered perfectly conducting, and second, the electric and magnetic fields within each slit are represented by their fundamental eigenmodes only. The results show that there is a close relationship between the zeros of the real and the imaginary parts of the determinants of certain characteristic matrices, and the spectral positions of the transmittance maxima and minima, respectively. Consequently, this method constitutes a practical and fast tool to accurately predict the relevant characteristics of the transmitted response of compound structures for normal and oblique incidence, without the complete solution of the scattering problem. This makes this model very useful for the design of compound structures for particular applications. The possibility of applying this simple model to other kinds of dual-period structures is also being investigated.

Acknowledgments

D S would like to thank Dr Marina Inchaussandague and Dr Ricardo Depine for stimulating and fruitful discussions. The author gratefully acknowledges partial support from Consejo Nacional de Investigaciones Científicas y Técnicas (CONICET grant PIP 5700), Universidad de Buenos Aires (UBA grants X283 and X208) and Agencia Nacional de Promoción Científica y Tecnológica (ANPCyT-BID 1728/OC-AR PICT 11-1785).

References

[1] Porto J A, García-Vidal F J and Pendry J B 1999 *Phys. Rev. Lett.* **83** 2845
[2] Ebbesen T W, Lezec H J, Ghaemi H F, Thio T and Wolff P A 1998 *Nature* **391** 667
[3] Astilean S, Lalanne Ph and Palamaru M 2000 *Opt. Commun.* **175** 265
[4] Takakura Y 2001 *Phys. Rev. Lett.* **86** 5601
[5] García-Vidal F J and Martín-Moreno L 2002 *Phys. Rev.* B **66** 155412
[6] Martín-Moreno L, García-Vidal F J, Lezec H J, Degiron A and Ebbesen T W 2003 *Phys. Rev. Lett.* **90** 167401
[7] Xie Y, Zakharian A R, Moloney J V and Mansuripur M 2004 *Opt. Express* **12** 6106
[8] Bravo-Abad J, Martín-Moreno L and García-Vidal F J 2004 *Phys. Rev.* E **69** 026601
[9] Benabbas A, Halté V and Bigot J-Y 2005 *Opt. Express* **13** 8730
[10] Xie Y, Zakharian A R, Moloney J V and Mansuripur M 2006 *Opt. Express* **14** 6400
[11] Gordon R 2006 *Phys. Rev.* B **73** 153405
[12] García-Vidal F J, Lezec H J, Ebbesen T W and Martín-Moreno L 2003 *Phys. Rev. Lett.* **90** 213901
[13] Cao H and Nahata A 2004 *Opt. Express* **12** 1004
[14] Beruete M, Campillo I, Dolado J S, Rodríguez-Seco J E, Perea E and Sorolla M 2004 *IEEE Antennas Wirel. Propag. Lett.* **3** 328
[15] Beruete M, Sorolla M, Campillo I and Dolado J S 2005 *IEEE Microw. Wirel. Compon. Lett.* **15** 286
[16] Lee J W, Seo M A, Kim D S, Jeoung S C, Lienau Ch, Kang J H and Park Q-H 2006 *Appl. Phys. Lett.* **88** 071114
[17] Skigin D C and Depine R A 2007 *Appl. Opt.* **46** 1385
[18] Lester M, Skigin D C and Depine R A 2008 *Appl. Opt.* **47** 1711
[19] Lester M, Skigin D C and Depine R A 2009 *J. Opt. A: Pure Appl. Opt.* **11** 045705
[20] Skigin D C and Depine R A 2005 *Phys. Rev. Lett.* **95** 217402
[21] Skigin D C and Depine R A 2006 *Opt. Commun.* **262** 270
[22] Skigin D C and Depine R A 2006 *Phys. Rev.* E **74** 046606
[23] Skigin D C, Loui H, Popovic Z and Kuester E F 2007 *Phys. Rev.* E **76** 016604
[24] Hibbins A P, Hooper I R, Lockyear M J and Sambles J R 2006 *Phys. Rev. Lett.* **96** 257402
[25] Ma Y G, Rao X S, Zhang G F and Ong C K 2007 *Phys. Rev.* E **76** 085413
[26] Navarro-Cía M, Skigin D C, Beruete M and Sorolla M 2009 *Appl. Phys. Lett.* **94** 091107
[27] Andrewartha J R, Fox J R and Wilson I J 1977 *Opt. Acta* **26** 69
[28] Medina F, Skigin D C and Mesa F 2008 *Proc. 38th European Microwave Conf.* vol 702
[29] Medina F, Mesa F and Skigin D C 2009 *IEEE Trans. Microw. Theory Tech.* submitted
[30] Gordon R 2006 *Phys. Rev.* B **73** 153405
[31] Quémerais P, Barbara A, Perchec J Le and López-Ríos T 2005 *J. Appl. Phys.* **97** 053507
[32] Skigin D C, Veremey V V and Mittra R 1999 *IEEE Trans. Antennas Propag.* **47** 376
[33] Fantino A N, Grosz S I and Skigin D C 2001 *Phys. Rev.* E **64** 016605
[34] Skigin D C, Fantino A N and Grosz S I 2003 *J. Opt. A: Pure Appl. Opt.* **5** S129